Winter 12-22-2022

HEAT STRESSED EXERCISE ELICITS SHIFTS IN COOLING STRATEGIES ACROSS BODY MASS IN TROPICAL SONGBIRDS

Kristen Dee Oliver
University of New Mexico - Main Campus

Kristen Oliver

Candidate

Biology

Department

This thesis is approved, and it is acceptable in quality and form for publication:

Approved by the Thesis Committee:

Christopher Witt , Chairperson

Jennifer Rudgers

Alexander Gerson

HEAT STRESSED EXERCISE ELICITS SHIFTS IN COOLING STRATEGIES ACROSS BODY MASS IN TROPICAL SONGBIRDS

By

KRISTEN D. OLIVER

B.A. Biology, Coker College, 2015

THESIS

Submitted in Partial Fulfillment of the Requirements for the Degree of

Master of Science

Biology

The University of New Mexico

Albuquerque, New Mexico

May, 2023

ACKNOWLEDGMENTS

I would like to thank my Advisor Dr. Christopher Witt for his trust, guidance, and constant encouragement throughout my time at UNM. I would also like to thank and acknowledge my two other committee members Dr. Jennifer Rudger, who has provided me with essential statistical help and guidance and Dr. Alexander Gerson for support in the physiology of this work and guidance of publication.

I would also like to thank my fellow co-workers, graduate students, and technicians that worked alongside me in the field in 2019 and 2020 on Mount Kinabalu.

A special thank you so Jani Sleutel for all her kindness, hard work, and patience working with me in the field. This project would not have been possible without her!

Last, but not least, I would like to thank all my fellow graduate students in the UNM biology department who have encouraged and supported me tremendously through this process. I would not have been able to do it without them.

Funding for this research was provided by the National Science Foundation (IOS-1656273).

HEAT STRESSED EXERCISE ELICITS SHIFTS IN COOLING STRATEGIES ACROSS BODY MASS IN TROPICAL SONGBIRD SPECIES

By

KRISTEN D. OLIVER

B.A. Biology, Coker College, 2015

M.S. Biology, University of New Mexico, 2023

Abstract

In resting animals, water use positively correlates with metabolic rate, for example smaller animals using proportionally more water per gram of body mass. However, animals also must endure heat and exertion, and evaporative cooling requires additional water use that may not scale similarly with body size. How evaporative water loss allometrically scales with body mass during heat-stressed exercise is poorly resolved, particularly for birds, yet is critically important for understanding the consequences of climate warming on the fitness of bird populations. Here, we evaluated how air temperature (T_a) influenced evaporative water loss during exercise ($EWL_{exercise}$) across tropical bird species that varied 18-fold in body mass (M_b). We also tracked changes in body temperature ($T_{b\ exercise}$) and metabolic rate during exercise ($MR_{exercise}$) to better

understand the physiological consequences of alternative scaling relationships between $EWL_{exercise}$ and M_b. Using push open-flow respirometry, we measured $EWL_{exercise}$, $MR_{exercise}$, and $T_{b\ exercise}$, across air temperatures from 15-30^{o}C in 12 species of passerines from a humid, subtropical forest in Kinabalu Park, Borneo, Malaysia. Across body masses of 6.5–116 g, larger species required more evaporative cooling and exhibited higher rates of evaporative water loss during activity at warm (>23^{o}C) air temperatures. Differences in $EWL_{exercise}$ across body masses were likely due to lower surface area -to-volume ratios of larger species. $T_{b\ exercise}$ were more labile with T_a in small species than in large species. Heat loading provided an alternative to water loss in small species, and led to the use of conductive cooling as an alternative to evaporative cooling. Larger birds were more susceptible to water loss during exertion at warmer air temperatures. This finding could help to explain the evolution toward smaller body sizes under Anthropocene warming, a widely reported phenomenon, and predict declines of larger-bodied birds under future climate warming.

TABLE OF CONTENTS

LIST OF FIGURES

LIST OF TABLES

Keywords:

Climate change; Allometry; Evaporative cooling; Air temperature; Exercise Metabolic rate; Body temperature; Hop-flutter wheel

Abbreviations:

T_a= Air temperature

M_b=Body mass

T_b= Body temperature

$T_{b\ exercise}$= Exercise body temperature

$MR_{exercise}$= Exercise metabolic rate

BMR= Basal metabolic rate

EWL= Evaporative water loss

$EWL_{exercise}$= Exercise evaporative water loss

TNZ = Thermal neutral zone

TEWL = Total evaporative water loss

INTRODUCTION

The logarithmic scaling of metabolic rate with log body mass is a foundational concept of physiological ecology. Max Kleiber established early on that the relationship of log metabolic rate with log body mass maintains a scaling exponent between 2/3 and ¾ (Kleiber, 1932). Variation in the allometry of metabolism has provided insight into the

potential effects of climate change on species populations (McKechnie et al., 2021). However, recent studies have indicated that in homeothermic endotherms, cooling capacities may be a more important driver in population declines due to anthropogenic climate change, than metabolic rate. We know that resting evaporative cooling responses illustrate a similar scaling exponent to the allometric scaling exponents of resting metabolic rates (Gavrilov, 2014, 2017; Hinds & MacMillen, 1985, 1986). But our understanding of how evaporative cooling allometry is impacted by air temperature is limited. Because it is well documented that air temperature can affect the amount of evaporative cooling an organism requires, measurements across body masses (M_b) are typically only compared at a single air temperature (T_a) (Dawson, 1982; Weathers, 1981; Wolf & Walsberg, 1996a). In fact, common practice is to compare measurements across species and body mass at a single T_a within the Thermal Neutral Zone (TNZ) where there is likely to be little additional influence of T_a (Gavrilov & V Gavrilov, 2019). Only a few studies on birds have looked at the effects of air temperature on the allometric relationship itself (Gavrilov, 2017; McKechnie et al., 2021; Gavrilov & V Gavrilov, 2019).

We expect T_a to impact the relationship of evaporative water loss across body mass based on a few comparative studies. For example, a recent study on birds looked at the allometric relationships of total evaporative water loss (TEWL) rates and percent of heat dissipated by evaporation during rest at two air temperatures: the upper critical temperature of the TNZ and the lower critical temperature of the TNZ (Gavrilov, 2017). At the higher T_a evaporative cooling was higher across all body masses (Gavrilov, 2017; McKechnie et al., 2021). However, our explicit understand of the influence of air

temperature on evaporative cooling allometry ends here. A more thorough test of air temperature impacts across body mass may be necessary to predict how species will respond to warming global air temperatures.

Measurements like the ones in the studies above are only conducted on resting animals and have limited application to the natural world given that activities such as flight and foraging are necessary to stay alive. However, increases in activity levels can also cause increases in total energy expenditure and accordingly evaporative cooling (Ettinger & King, 1980). During intense exercise in both domestic fowl (Warren SSL strain; M_b= 2.2kg) and budgerigars (*Melopsittacus undulatus*; M_b= 33.5g) respiration rate increased while lung tidal volume decreased resulting in shorter and faster breaths, often known as panting (Brackenbury, 1984). By creating these rapid short breaths individuals are attempting to maximize evaporative cooling capacities, in addition to adjusting for increased tissue gas exchange needs. However in White-necked ravens (*Corvus cryptoleucus*; M_b= 0.48kg), T_b and respiratory frequencies measurements both rose during steady state flight with increasing T_a, but metabolic rate did not increase with T_a (Hudson & Bernstein, 1981). Without additional heat gain of metabolic rate as T_a increased, T_b can only increase due to environmental heat gain, indicating that these short fast breaths are not enough to dissipate all heat being gained at the highest T_a (34^{o}C).

Evaporative cooling is one of the most effective methods of thermoregulation in birds, but not the only known mechanism. In the White-necked Ravens, the ratio of total evaporative heat loss to heat production was found to be 0.48 during flight at 33^{o}C for the 0.48 kg ravens. Compared to smaller Budgerigars (M_b=33.5g) and Starlings (*Sturnus vulgaris*; M_b= 74g) these species showed similar values but at higher T_a, 0.47 at 37^{o}C in

Budgerigars, and lower values than the Ravens at similar T_a, 0.29 at 28^oC in Starlings (Torre-Bueno, 1978; Tucker, 1968). This demonstrates that there could be differences in how species of different sizes rely on evaporative cooling responses during activity. Another documented form of thermoregulation in avian species is facultative hyperthermia. This is a process in which an animal stores body heat creating a gradient between T_a and T_b (Gerson et al., 2019; McKechnie & Lovegrove, 2002) to promote dissipation of heat from the body to the environment without additional energy expenditure. This strategy can be a water saving mechanism as T_a moves above the upper critical temperature, particularly for small animals with high surface area to volume ratios (Weathers, 1981). It is possible that the smaller Budgerigars and starlings are using this mechanism, but without simultaneous T_b, and EWL measurements this theory can't be well supported.

Many of the studies explicitly measuring simultaneous physiological responses to heat stressed exercise were conducted typically on one species at a time, of only a few individuals (1-7; Aulie, 1971; Hudson & Bernstein, 1981; Torre-Bueno, 1978; Tucker, 1968). John Brackenbury reviewed the physiological responses of birds to flight and running in 1984 of literature published up to that point, but there is no direct comparison of the effects of T_a across body mass during activity (Brackenbury, 1984). Therefore, an explicit understanding of how evaporative cooling rates (EWL), T_b, and metabolic rate (MR) vary across M_b and T_a during activity has not yet been established. Our study sought to fill this gap in our knowledge by taking simultaneous measurements of T_b, EWL, and MR for all individuals across a range of T_a and M_b.

Here we investigate the subsequent effects on body temperature during exercise ($T_{b\ exercise}$) and metabolic rate during exercise ($MR_{exercise}$) with a focus on evaporative water loss ($EWL_{exercise}$) rates as a potential limiting mechanism across M_b and T_a. To do this we took simultaneous measurements of $MR_{exercise}$, $EWL_{exercise}$, and $T_{b\ exercise}$ across a range of 12 bird species and body sizes using open flow respirometry in a metabolic chamber constructed as a hop flutter wheel. We hypothesized that smaller species will rely on heat storage or facultative hyperthermia rather than evaporative cooling during heat stressed activity because of their higher surface area to volume ratio or lack of threat from thermal inertia. While larger species have lower surface area to volume ratios and therefore cannot lose heat as efficiently through conduction or convection. Exercise and increasing T_a could compound heat gain in larger species and disrupt their ability to perform and/or thermoregulate during activity due to thermal inertia. Therefore, we also hypothesize that the effects of T_a on EWL in larger species may be exacerbated during exercise and larger species will rely on higher evaporative water loss rates to maintain T_b below lethal limits. Few studies have been conducted on avian species during exercise at varying air temperatures. Those that have, have not measured metabolic rate, body temperature, and evaporative cooling responses directly and simultaneously across body sizes. This leaves a significant gap in our understanding of how species are thermoregulating during hyperthermic exercise; A key factor when considering how species might respond to climate change.

Much focus has been placed on increases in environmental air temperature (T_e) as a result of global climate change. With respect to potential ecological effects of increasing T_e, one hypothesis that has gotten a lot of attention over recent years predicts

that increases in T_e are correlated with overall decreases in body size of entire animal populations (Gardner et al., 2011, 2018; Prokosch et al., 2019; Sheridan & Bickford, 2011; Van Buskirk et al., 2010; Weeks et al., 2020). A Few studies have even detected rapid changes in current population body mass and morphology correlated with T_e (Prokosch et al., 2019; Van Buskirk et al., 2010). Selective pressures, such as survival probability, have also been correlated to increases in T_e and the resulting decrease in body size. Within a population of Mountain wagtails (*Motallica clara*) lighter individuals were shown to have higher adult survival probability under higher T_e conditions while larger individuals demonstrated better adult survival under lower T_e conditions (Prokosch et al., 2019). These effects of T_e on survival probability demonstrate a potentially very powerful selective pressure. By looking at the effects of T_a on physiological responses of birds during activity in a controlled lab setting, we may gain a better understanding of how increases in T_e could translate to energetic demands of foraging, migration, and reproduction across body sizes. While understanding that additional energetic demands have been linked to decreases in average brood size, juvenile survivorship, adult survivorship, and increases in time between successive broods (Lemon, 1993). All of which are potentially strong selective pressures towards smaller body sizes and lower energetic demands on daily energy budgets and activities.

Our study investigates the allometric scaling of exercise MR, EWL and T_b in response to changes in Ta across a range of body masses from 6.5g to 116g in species from a mid-elevation tropical ecosystem. Only a few studies have been conducted on species in tropical environments (Muskett et al., 2020; Pollock et al., 2019, 2021; Scholander et al., 1950; Weathers, 1997). Some of these studies have found that bird

species inhabiting more tropical environments have lower evaporative cooling responses than species found in more desert environments (Noakes et al., 2016; Tieleman et al., 2003). Our data will also contribute to the small pool of literature on how tropical species might respond to climate change. To address these questions, we measured exercise metabolic rates, body temperature, and evaporative water loss rates across ecologically relevant air temperatures (15-30^{o}C) and across a variety of species and body sizes found on Mount Kinabalu in Borneo, Malaysia.

METHODS

Study site and species

Our study site was located at the headquarters area of Kinabalu park (1,450 - 1,950m of elevation), a mid-elevation tropical rainforest in Sabah, Borneo, Malaysia. We measured Maximal metabolic rates and resting metabolic rates between February – June 2019 and Basal metabolic rates between February-March and May-June of 2020. We sampled metabolic rates from 12 species in 9 Passerine families (Table 1: IOC World Bird List 12.1).

Bird handling protocols

We captured birds using mist nets and playback recordings to increase capture rates and reduce bycatch. Upon capture, we extracted birds and held them in cloth bags until time for banding. Using the protocols described in Martin et al., 2017 we banded each individual and collected standard morphological measurements (e.g., body mass, wing chord, tarsus, bill measurements, etc.). Birds were then transported to a separate

facility and placed in holding chambers in a quiet, temperature-controlled room with ambient temperatures within their thermal neutral zone (≈ 30ºC).

We hand fed each bird every two hours unless individuals ate supplied food on their own in the holding chambers. At this time, we also hand watered every individual in order to ensure appropriate water intake. To reduce possible variations in respiratory quotients between individuals, we measured $MR_{exercies}$ on birds in a postabsorptive state by withholding food for 1-2 hours, before placement into the metabolic chamber. For species with body masses above 20g, the waiting time was 2 hours (Walsberg and Wolf, 1995). Individuals utilized in BMR measurements were fed all day until their last feed at sunset just before being placed in a metabolic chamber.

Body Temperature Measurements

We used Passive integrated transponder (PIT) tags (BioMark®, Boise, ID, USA. BioThermo13, accuracy ± 205 0.02°C (Whitfield et al., 2015) to measure core body temperature in seven species with average M_b › 10g (Table 1). PIT-tags were implanted via intraperitoneal injection using a tag injector (Biomark® MK10). During $MR_{exercise}$ measurements, body temperature was measured continuously via a Biomark® HPR Plus reader and antenna. Temperatures corresponding to BMR measurements were taken as rectal temperatures before and after metabolic trials.

Experimental Protocols

Exercise Metabolic rates and Exercise Evaporative water loss

We measured CO_2 production and total evaporative water loss (EWL) using a push open flow respirometry system inside a custom-built hop-flutter wheel to elicit $MR_{exercise}$. Outside air was pushed into the system using a ½ hp oilless air compressor with an attached air dryer and regulator. To ensure minimal pressure fluctuations from the air compressor, we first pushed air into a 33L PVC carboy. From the carboy, air was pushed through two drying columns, the first containing silica gel and the second Drierite™. We then pushed the dried air into two mass flow controllers (Alicat scientific, Tucson, AZ, USA. MC-1SLPM, MC-30SLPM, Mass Flow Controller, accuracy: ± 0.8% of reading + 0.2% of full scale). One mass flow controller was set to 0.5 L min^{-1} STP and pushed air to one CO_2 H_2O^{-1} gas analyzer (Li-Cor, Lincoln, NE, USA, model 840A, accuracy ± 1ppm CO2, ±0.01% reading 179 for H2O) to measuring a continuous baseline. The second mass flow controller regulated airflow to the chamber at 10 L min^{-1}. Our hop-flutter wheel was a custom-built airtight chamber (UNM Mechanical Engineering Machine Shop, Albuquerque, NM, USA) with aluminum panels running the width of the cylinder and clear plexiglass walls on either side, one with a single access door. We mounted the hop-flutter wheel using aluminum A-frame plates and bearings to an aluminum base plate that also housed a motor attached to the back of the wheel via a pulley wheel and belt system. The hop-flutter wheel was 24 cm in height and 900 cm in diameter measuring a total volume of 68.85L. Air was pushed through diffuser fittings attached to the plexiglass both entering and exiting the chamber, which allowed for complete mixing of the air within the large chamber volume. We measured subsampled air from the outtake of the chamber using a second CO_2 H_2O^{-1} gas analyzer. Ambient T_a was measured using a thermocouple inserted into the outtake tubing of the chamber. We

acquired data through a National Instruments ™ DAQ (National Instruments ™, Austin, TX, USA) that hosted connections from the mass flow controllers, gas analyzers, and thermocouples. All data interpreted through the DAQ and the BioMark receivers were visualized and saved using LabVIEW (National Instruments ™, Austin, TX, USA).

The hop-flutter wheel was housed inside a custom-built environmental chamber made of aluminum framing and styrofoam siding. T_a was regulated using a Peltier device (model AC-162, TE Technology Inc., Traverse City, MI, USA) and a custom-built controller. Our experimental design was to measure $MR_{exercise}$ at a single T_a setpoint for each individual, where T_a ranged between 15-30^{o}C for each species. We attached contact paper and straws to the inside of the wheel to provide perches and traction for the birds during $MR_{exercise}$ trials. For some trials, we added 1-2 Ping-Pong balls to encourage movement during $MR_{exercise}$ trials. Each bird entered the chamber and was given a 30-50 min acclimation period while the environmental chamber was covered with a bed sheet to darken the chamber and help keep the birds calm. After the acclimation period, we ran $MR_{exercise}$ trials for 5 minutes, controlling wheel movement to encourage the birds to move and sustain maximal activity. Birds that would not exercise for the full trial period were not included in the data set. All birds that were included in this data set exhibited wing drooping and panting, indicating that our trials elicited maximal exertion. We counted hops for 1-minute intervals starting at the start of the trial and then every other minute after, resulting in three subsamples of the entire trial. We considered hops to be associated with a jump or flutter in which the bird was encouraged to move its wings and elicit the movement of the pectoralis muscle.

We observed a lethal limit in one species, Mountain Wren-babblers (*Gypsophila crassa*), after exercise trials held at or above 30°C (n=3). A maximum of three consecutive trials were run on each bird. The first trial was selected for calculation of $MR_{exercise}$ and $EWL_{exercise}$. Consecutive trials were part of a separate question and were therefore not included in this analysis other than performing instantaneous calculations.

Basal Metabolic rates and Evaporative Water loss

We measured CO_2 production and total evaporative water loss using a push open flow respirometry system. Similar to above, we pushed dried air to four mass flow controllers (Alicat scientific, Tucson, AZ, USA. MC-1SLPM, MC-5SLPM, Mass Flow Controller, accuracy: ± 0.8% of reading + 0.2% of full scale) controlling flow to each chamber with flow rates ranging from 0.2-1.5 L min^{-1} STP. Metabolic chambers were airtight clear, plastic containers ranging in size from 1.7-5L in volume. Wire platforms made from PVC coated chicken wire were provided for the birds to rest, above a thin layer of olive oil coating the bottom of the chamber to prevent water and carbon dioxide contamination from fecal matter. Excurrent air from each metabolic chamber flowed to a multiplexer port (model MUX3-1101-18M, Sable Systems, North Las Vegas, NV, USA) which allowed subsampling of air to a CO_2 H_2O^{-1} analyzer (Li-Cor, Lincoln, NE, USA, model 840A, accuracy ± 1ppm CO2, ±0.01% reading 179 for H2O) . We automated the multiplexer to switch between chambers every 2 minutes with baseline measurements occurring once every 10 minutes. Metabolic chambers were housed in a modified ice chest mounted with a Peltier device to control T_a within the thermoneutral zone for all species sampled (typically between 28-30°C). We determined thermoneutrality by performing overnight temperature trials for each species, where we slowly adjusted

temperatures to identify which T_a lowered metabolic output to a minimum. To measure T_a, we used thermocouples sealed into each chamber and voltages were interpreted using a Sable Systems TC-2000 (Sable Systems, North Las Vegas, NM, USA). We acquired and visualized our data using a Sable Systems UI2 (Sable Systems, North Las Vegas, NM, USA) and Expedata software (Sable Systems, North Las Vegas, NM, USA). All animals were sampled during their rest phase and experiments typically lasted 4-6 hours to ensure we were obtaining the lowest possible resting values.

Metabolic calculations and Statistical analysis

To estimate $MR_{exercise}$ and $EWL_{exercise}$ we used R version 3.6.3 (R Core Team, 2020) to organize, clean, extract and calculate our metabolic measurements. We first removed electrical noise spikes, subtracted baseline levels, and smoothed CO_2 and H_2O values. Smoothing was performed using a simple moving average in preparation for instantaneous transformation. Using impulse response curves created by blowing into the intake tube of the chamber, we filtered our data to only analyze individuals with recording times at least as long as the measured washout of the impulse response curve. Chosen for its repeatability and demonstration of accuracy with short measurements, we used the Tikohnov regularization method to perform an instantaneous transformation (Pendar et al., 2016; Pendar & Socha, 2015)(see Appendix A & B). Using MATLAB Release 2018b (The MathWorks, Inc., 2018) and code derived from Pendar et al., 2016 we calculated instantaneous values for CO_2 and H_2O. We validated these calculations in the lab using a zero gas and room air (see Appendix A & B). We estimated $MR_{exercise}$ and $EWL_{exercise}$ by selecting the highest 2-minute rolling mean of CO_2 production found 30

seconds after the start of the trial and 30 seconds before the end of the trial. We selected $T_{b\ exercise}$ as the last PIT-tag read at least 30 seconds before the end of the 5 min exercise trial.

Data collected for BMR was exported from Expadata into R v3.6.3 for cleaning and analysis (R Core Team, 2020). Within these files, we estimated BMR by selecting the lowest 1-minute rolling mean. For birds weighing less than 20g this 1-minute rolling mean was selected at least 60 minutes after the bird entered the chamber, while estimates for birds over 20g were selected at least 120 minutes after entering the chamber to ensure a postabsorptive state. Because BMR measurements were taken in different individuals in a different year than $MR_{exercise}$ measurements, we averaged BMR within species for comparison to $MR_{exercise}$.

Using our selected sample periods we calculated whole animal $MR_{exercise}$, BMR and corresponding EWL using equations 10.5 and 10.9 from Lighton (2008). We assumed all animals were post absorptive during the time the values were estimated, and therefore assumed a respiratory quotient (RQ) of 0.71 (Walsberg & Wolf, 1995). We calculated metabolic rates by converting rates of CO_2 production to metabolic heat production using a thermal equivalent of 27.8 J ml^{-1} CO_2 (Withers, 1992). Similarly we converted EWL to metabolic heat loss (mW) using 2.43kJ g^{-1} (Lighton, 2008). We calculated evaporative heat dissipation ($EHD_{exercise}$) as $EWL_{exercise}/MR_{exercise}$.

To determine if there was a phylogenetic signal in all of our measured variables, we used Pagel's Lambda and Blomberg's K. We used a phylogeny produced by generating a consensus tree derived from 100 trees downloaded on Birdtree.org from a (Hackett et al., 2008) backbone. We then tested for a phylogenetic signal in averaged

values of BMR for each species and average $MR_{exercise}$, $EWL_{exercise}$, and $T_{b\ exercise}$ at both high ($T_a \geq 27^oC$) and low ($T_a \leq 19^oC$) temperatures for each species. Pagel's lambda and Blomberg's K tests revealed no phylogenetic signal on either end of the temperature range for all physiological variables (see Appendix G). Therefore, we used non-phylogenetic regressions and analyses going forward.

To evaluate the relationship of M_b scaling of $EWL_{exercise}$ with changing T_a we fit a linear mixed-effects model (package *lme4* v1.1-14: (Bates et al., 2015) to our data and used an AIC model selection process to compare model fit. We visualized this relationship using the *visreg2d* function from the *visreg* v2.7.0 package (Breheny & Burchett, 2017). We used the same model selection procedures to evaluate the relationship of $T_{b\ exercise}$ with T_a and M_b during exercise, $MR_{exercise}$ with T_a and M_b, and $EHD_{exercise}$ with T_a and M_b to better understand what could be driving the relationships found in our model of $EWL_{exercise}$ with T_a and M_b.

RESULTS

Our dataset provides insight into how species of different body masses respond physiologically to exercise at varying air temperatures. We measured $MR_{exercise}$ in 187 individuals with sample sizes for each species ranging from 5-29 individuals. BMR was measured in 99 individuals with sample sizes ranging from 2-18 individuals per species (Table 1). Our largest measured species was the Bornean Whistling Thrush with an average weight of 116 g. $MR_{exercise}$ values for the Bornean Whistling Thrush ranged from 7.035W to 9.735W which is 8.13xBMR to 12.27xBMR across air temperatures. Our smallest study species measured was the Yellow-breasted Warbler with an average

weight of 6.5g. The Yellow-breasted Warbler produced $MR_{exercise}$ values ranging from 0.494W to 1.115W which is 3.51xBMR to 8.11xBMR across air temperatures. The species with the most labile body temperature was the Chestnut-crested Yuhina with a body temperature values ranging from 38.6°C to 46.3°C across air temperatures during $MR_{exercise}$ trials. For one species, the Mountain Wren-babbler, we observed a possible lethal limit after exercise at $T_a \geq 30$°C (n=3). We measured $MR_{exercise}$ values for Mountain Wren-babblers to be between 1.786W to 4.430W which is 5.40xBMR and 11.43xBMR while their body temperature values fluctuated from 39.8°C to 45.8°C across air temperatures during exercise. We believe that this lethal limit could be a result of high water demands during activity at high air temperatures. $EWL_{exercise}$ values for the Mountain Wren-babblers ranged between 0.389W to 5.016W which is 4.87xBMR and 55.00xBMR across air temperatures with the highest value occurring at 30°C. While our largest species, the Bornean Whistling Thrush, showed $EWL_{exercise}$ values ranging from 2.013W to 10.877W which is 7.88xBMR to 27.97xBMR.

Exercise evaporative water loss rates across M_b and T_a

AIC model selection indicated the most well supported final model with $EWL_{exercise}$ as the response variable contained T_a, log M_b and average hops as fixed effects and species as a random effect (Appendix C). We found a significant positive relationship in log $EWL_{exercise}$ rates with T_a ($\beta = 0.03$; $P < 0.001$), log M_b ($\beta = 1.02$; $P < 0.001$), and average hops ($\beta = 0.01$; $P = 0.005$) during exercise across species (Figure 1; Table 2; conditional $R^2 = 0.725$). In this model our fixed effects accounted for the majority of the variation in the data with a marginal R^2 of 0.685.

Exercise body temperature across M_b and T_a

We measured $T_{b\ exercise}$ for 133 individuals from 10 species large enough to insert pit tags (>10g). Our AIC model selection indicated a best fit model of $T_{b\ exercise}$ as the response variable with fixed effects of T_a, M_b, and their interaction term and species as a random effect (Appendix D). This model specifies that $T_{b\ exercise}$ has an inverse heteroscedastic relationship with T_a and M_b as seen in Figure 2 (conditional $R^2 = 0.60$). Specifically, this model indicated a significant positive relationship between $T_{b\ exercise}$ and T_a ($\beta = 0.44$; $P < 0.001$) while the interaction term of T_a and M_b demonstrated a significant negative relationship (Figure 3; $\beta = -0.08$; $P = 0.0060$) when all other variables are held constant. There was no significant relationship between $T_{b\ exercise}$ and log M_b ($\beta = 1.78$; $P = 0.8246$), which is to be expected given the scope of body masses this study covers. The negative relationship traditionally documented with avian body mass and T_b is seen across large scale differences in body mass (1-100,000g; 5 orders of magnitude) while our samples encompass a much smaller scale difference in body mass (12-116g; 1 order of magnitude) (McNab, 1966). The fixed effects of this model, T_a and M_b, accounted for just under the majority of the variation within the data with a marginal R^2 value of 0.49 (Table 2).

Exercise metabolic rates across M_b and T_a

Our AIC model selection determined a best fit final model with $MR_{exercise}$ as the response variable with T_a, log M_b, the interaction term of T_a and log M_b, and average hops as fixed effects and species as a random effect (Appendix E). This model indicates a

significant positive relationship between log $MR_{exercise}$ and log M_b ($\beta = 0.82$; $P < 0.001$) as well as a small significant positive relationship with log $MR_{exercise}$ and T_a ($\beta = 0.01$; $P = 0.02$) and log $MR_{exercise}$ and average hops ($\beta = 0.01$; $P < 0.001$) when all other variables are held constant (Figure 3). There was a slight negative relationship with log $MR_{exercise}$ and the interaction term of T_a and M_b though it was not statistically supported ($\beta = -0.01$; $P = 0.139$). The fixed effects of this model accounted for the majority of the variation in $MR_{exercise}$ as apparent by the small differences in R^2 values (marginal $R^2 = 0.86$, conditional $R^2 = 0.89$; Table 2).

Evaporative heat dissipation across M_b and T_a

AIC model selection determined a best fit model with our calculated $EHD_{exercise}$ as the response variable with T_a and log M_b as fixed effects and species as a random effect (Appendix F). This model indicated slight positive relationships between $EHD_{exercise}$ and T_a ($\beta = 0.01$; $P < 0.001$) and $EHD_{exercise}$ and M_b ($\beta = 0.21$; $P = 0.008$) that were statistically significant when all other variables are held constant (Figure 4). However, this model did not account for the majority of the variation in the data based on R^2 values (marginal $R^2 = 0.13$, conditional $R^2 = 0.23$; Table 2). We speculate that this could be due to a variety of possible explanations. The derived nature of this calculation could contribute to overall noise, and/or the effects on large species are washed out due to our small sample sizes of large species across air temperature.

DISCUSSION

We found that larger species engage in higher total evaporative cooling (β =1.02; $P < 0.001$) during activity at high air temperatures ($\beta = 0.03$; $P < 0.001$) than smaller species (Figure 1), but the relationship between $EWL_{exercise}$ and T_a was the same across body mass. The relationship between $EWL_{exercise}$ and T_a likely did not change across body masses because of inherent differences in surface area to volume ratios and thermal inertia in smaller species vs. larger species. Body temperatures were more labile in smaller species (Species ≤ 26g: $T_{b\ exercise}$ range 38.3 - 46.3^{o}C) allowing for convective cooling and possibly conservation of water during activity. $MR_{exercise}$ was slightly higher at high T_a across body sizes though the interaction of M_b and T_a showed a negative relationship. It is possible, however, that larger sample sizes of our larger study species would have allowed for more statistical support for this interactive relationship. We hypothesize that these relationships with $MR_{exercise}$ are likely a result of thermoregulatory constraints of $EWL_{exercise}$ and $T_{b\ exercise}$. Supported for this hypothesis was also apparent in high values of $EHD_{exercise}$ of our larger species. Lethal limits were detected in only one of our study species and could indicate a species at risk as air temperatures rise.

Rate of evaporative water loss increases with M_b and T_a

Larger species could be at risk of overheating during exercise without their increased ability to evaporatively cool. Our model of $EWL_{exercise}$ across M_b and T_a estimated a significant positive slope (M_b : β =1.02; $P < 0.001$; T_a : $\beta = 0.03$; $P < 0.001$) in $EWL_{exercise}$ rate during activity (Figure 1). This supports our hypothesis that larger species would rely on higher EWL rates to regulate T_b below lethal limits. This hypothesis is further supported by the narrow range of $T_{b\ exercise}$ seen in our largest

species, the Bornean Whistling Thrush (40.8 - 43.1^{o}C) (Figure 2). However, our results during exercise demonstrated these similar changes in EWL and T_b at relatively low T_a compared to those measured in studies of individuals at rest (Gavrilov, 2017; McKechnie et al., 2021; Weathers, 1981). This could be a result of compounded heat effects of $MR_{exercise}$ and T_a and the determinants of thermal inertia as T_b increases. Thermal inertia has the potential to have a higher impact on larger species than smaller species due to differences in surface area to volume ratios and its effects on efficient conductive cooling (Wolf & Walsberg, 1996b). Larger species could be at a higher risk of overheating while exercising because dissipating heat passively is not an effective means of cooling and would not counteract the thermal inertia of their body temperature. Therefore, individuals of larger species must rely heavily on EWL to thermoregulate during exercise as is supported by our model for $EHD_{exercise}$ (Figure 4). Larger individuals elicited $EHD_{exercise}$ values higher than 1 at the highest air temperatures, indicating evaporative cooling rates higher than the heat being produced by metabolic rate along. These high $EHD_{exercise}$ values could be a result of the income of a significant heat load from the environment. However, the $T_{b\ exercise}$ measurements of these larger individuals are still slightly elevated and could indicate that these high evaporative cooling rates are still not enough to lower $T_{b\ exercise}$. This could be the approach of a limit in physiological function, but more data is needed at higher T_a and/or higher body masses to definitively say.

Hyperthermic savings in small species

Smaller species face fewer challenges with passively cooling than larger species and could benefit from water savings because of their high surface area to volume ratio.

Our models of $EWL_{exercise}$ and $T_{b\ exercise}$ both suggest that smaller individuals perform better than larger species during strenuous activity at high temperatures. Smaller species demonstrated extremely labile $T_{b\ exercise}$ measurements with extremes at both ends of the T_a range (Species ≤ 26g: $T_{b\ exercise}$ range 38.3 - 46.3^{o}C). In support of our hypothesis that smaller species could use facultative hyperthermia to conductivly cool our data shows that smaller species allow $T_{b\ exercise}$ to maintain a high $T_{b\ exercise}$-T_a gradient, benefiting from passive conductive cooling from the bird to the environment. Conductive cooling is a more water efficient way of cooling than the alternative, evaporative cooling (Gerson et al., 2019). Due to the larger surface area to volume ratios of smaller species they likely can conserve water during activity at high T_a through this mechanism of passively cooling, as long as T_a remains below T_b. This is also supported by low $EHD_{exercise}$ values in smaller species across T_a compared to $EHD_{exercise}$ values of larger species (Figure 4). Meaning that smaller species are producing more heat through metabolic heat production than they are evaporating, seen again by the elevated $T_{b\ exercise}$. All of which supports our hypothesis that smaller species would rely on passive means of cooling rather than increases in EWL to regulate $T_{b\ exercise}$ at higher air temperatures. However, this ability to transfer heat to the environment possibly works against our smaller individuals at lower values of T_a, as those species showed the lowest $T_{b\ exercise}$ measurements at temperatures below 19-20^{o}C. This is likely due, again, to the high surface area to volume ratios of smaller species and large $T_{b\ exercise}$-T_a gradients at these temperatures, which results in these species losing heat to the environment faster than their $MR_{exercise}$ can generate.

Possible insight into shrinking body size

With the support of our two hypotheses could come insight into the energetic selective pressures of T_a and T_e on body size in current and future climates. If water requirements and energetic requirements are lower for smaller species because of their ability to passively cool through conduction, then this could support the possibility of selection towards smaller body sizes. Though the savings may seem small in our experiment, if considered within the context of foraging for migration or reproductive efforts, the selective pressure towards a smaller body size could be much larger as T_e continues to rise. Not unfathomable, as additional energetic demands have been linked to decreases in average brood size, juvenile survivorship, adult survivorship, and increases in time between successive broods in lab experiments (Lemon, 1993). All these changes in breeding performance are potentially very strong selective pressures towards smaller body sizes and less energetic demands on daily energy budgets. Within the context of our study species it is reasonable to believe that the selective pressure would act on the cost of reproduction and possibility of nestling survival as these species often experience high predation rates and the possibility to nest year round compounding any effects on daily energy expenditure to a year round issue (Martin et al., 2015).

Microhabitat and lethal limits

In our data set we found significant variation in thermoregulatory strategies during exercise across body sizes. Field observations showed that all our study species appeared physically exhausted after any amount of activity at our highest tested air temperatures ($\geq 30^{o}$C). One species, the Mountain Wren-babbler, indicated a lethal limit after exercise at the highest temperatures. This finding was intriguing given that

temperatures at this study site can reach highs of 30-32^{o}C. We speculate that due to the understory and almost ground dwelling nature of this species, they may not experience much daily temperature fluctuation (Collar & Robson, 2021; Slevin et al., 2020). Therefore, it is possible that this species is acclimatized to a much cooler microclimate and less active flapping flight than the rest of our study species. Additional support for this theory can be seen in the $T_{b\ exercise}$ values of a more canopy dwelling and active species, the Chestnut-crested Yuhina (*Staphida everetti*). The Yuhinas demonstrated the greatest range of body temperatures of any of our species (38.6 – 46.3^{o}C), and are well known for rapidly foraging and flying in the mid to upper canopy of the forest, yet also nesting in the cool mossy banks of the forest floor (Myers, 2009). Gaining them exposure to a wider variety of microclimates and temperatures during their daily activities. However, this species was also one of the smallest species we could internally pit-tag, yet not the smallest, and therefore this could also be a side effect of having a larger surface area to volume ratio. Though this theory for the large range in $T_{b\ exercise}$ is contradicted by the fact that the smallest pit-tagged species, the White-throated Fantail (*Rhipidura albicollis kinabalu*) demonstrated a slightly small $T_{b\ exercise}$ range from 38.3- 45^{o}C. We are just beginning to understand the importance of microhabitats on thermoregulatory costs (Riddell et al., 2021; Walsberg, 1993), and it would be interesting to further explore these effects of potential microhabitat influence through exercise physiology as a possible stronger selective pressure than resting physiology.

It would be negligent, however, not to recognize that this possible lethal limit in Mountain Wren-babblers could also be an effect of the demonstrated overwhelm and stress induced by the overall experimental process, and it is possible the true thermal

limit is actually higher. However, individual Wren-babblers run at temperatures below 30^{o}C had no issues being released after their trials.

Caveates in evaporative cooling and humidity

In our experiments for this dataset, we measured $EWL_{exercise}$ by drying the air going into the chamber and measuring the change H_2O of the excurrent air. This method is effective for accurately measuring the amount of water individuals are losing to evaporatively cool their bodies. However, this method may not be the most biologically accurate way to take this measurement on our study system. Though we found significant relationships between $EWL_{exercise}$ vs. M_b vs. T_a, this relationship may differ in humid climates such as the climate these species live in. Previous studies have found that humidity decreases the efficiency of evaporative cooling, potentially meaning that our findings have overestimated the extent to which these species are capable of evaporative cooling during work at high air temperatures (Gerson et al., 2014; van Dyk et al., 2019). Despite this, our findings are consistent with other studies looking at heat dissipation during exercise in species typically found in arid climates (Aulie, 1971; Hudson & Bernstein, 1981).

Future Directions

Future studies looking at the effects of humidity on these types of measurements would be key in understanding the application of this data to the natural world, especially because more arid environments are responding differently to climate change than humid ones. Additional studies looking at how these coping mechanisms vary across habitat

types and life history strategies will provide key insight into which species are of most concern for experiencing downstream effects of the physiological stressors related to climate change. Lastly, data sets and models like these can be utilized in further predictive models to quantify the population level effects of climate change.

Conclusions

From the data presented here, we conclude that activity data is key for understanding the effects of T_a on birds in a rapidly changing climate. Our data indicates that larger species may experience additional costs associated with activity at higher T_a due to increased cooling requirements. Furthermore, smaller species are better equipped to cope with activity at higher temperatures using passive conductive cooling and a labile T_b. This sheds light on the potential effects of climate change on these tropical species and how body size may impact the magnitude of this effect. With one species demonstrating a previously unknown lethal limit after activity at only 30^{o}C, a relatively low T_e, this is a good indication that more data is needed on how species respond and cope with activity at higher temperatures. Additional water requirements associated with flying, foraging, reproduction, and predator avoidance may lead to downstream effects of reduced reproductive output. Therefore, passive cooling and reduced water requirements could result in higher selective pressures towards smaller body masses as T_e continues to rise.

REFERENCE

Aulie, A. (1971). Body temperatures in pigeons and budgerigars during sustained flight. *Comparative Biochemistry and Physiology Part A: Physiology*, *39*(2), 173–176. https://doi.org/10.1016/0300-9629(71)90074-0

Bates, D., Mächler, M., Bolker, B., & Walker, S. (2015). Fitting Linear Mixed-Effects Models Using **lme4**. *Journal of Statistical Software*, *67*(1). https://doi.org/10.18637/jss.v067.i01

Brackenbury, J. (1984). Physiological Responses Of Birds To Flight And Running. *Biological Reviews*, *59*(4), 559–575. https://doi.org/10.1111/j.1469-185X.1984.tb00414.x

Breheny, P., & Burchett, W. (2017). Visualization of Regression Models Using visreg. *The R Journal*, *9*(2), 56. https://doi.org/10.32614/RJ-2017-046

Collar, N., & Robson, C. (2021). Mountain Wren-Babbler (Gypsophila crassa). In S. M. Billerman, B. K. Keeney, P. G. Rodewald, & T. S. Schulenberg (Eds.), *Birds of the World*. Cornell Lab of Ornithology. https://doi.org/10.2173/bow.mowbab1.01.1

Dawson, W. R. (1982). Evaporative losses of water by birds. *Comparative Biochemistry and Physiology Part A: Physiology*, *71*(4), 495–509. https://doi.org/10.1016/0300-9629(82)90198-0

Ettinger, A. O., & King, J. R. (1980). *TIME AND ENERGY BUDGETS OF THE WILLOW FLYCATCHER (EMPIDONAX TRAILLII) DURING THE BREEDING*

SEASON. *97*, 14.

Gardner, J. L., Peters, A., Kearney, M. R., Joseph, L., & Heinsohn, R. (2011). Declining body size: A third universal response to warming? *Trends in Ecology and Evolution*, *26*(6), 285–291. https://doi.org/10.1016/j.tree.2011.03.005

Gardner, J. L., Rowley, E., de Rebeira, P., de Rebeira, A., & Brouwer, L. (2018). Associations between changing climate and body condition over decades in two southern hemisphere passerine birds. *Climate Change Responses*, *5*(1), 2. https://doi.org/10.1186/s40665-018-0038-y

Gavrilov, V. M. (2014). Ecological and Scaling Analysis of the Energy Expenditure of Rest, Activity, Flight, and Evaporative Water Loss in Passeriformes and Non-Passeriformes in Relation to Seasonal Migrations and to the Occupation of Boreal Stations in High and Moderate Latitudes. *The Quarterly Review of Biology*, *89*(2), 107–150. https://doi.org/10.1086/676046

Gavrilov, V. M. (2017). Total Evaporative Water Loss in Birds at Different Ambient Temperatures: Allometric and Stoichiometric Approaches. *Zoological Studies*, 16.

Gavrilov, V. M., & V Gavrilov, V. (2019). Scaling of total evaporative water loss and evaporative heat loss in birds at different ambient temperatures and seasons. *International International Journal of Avian & Wildlife Biology*, *4*(2). https://doi.org/10.15406/ijawb.2019.04.00150

Gerson, A. R., McKechnie, A. E., Smit, B., Whitfield, M. C., Smith, E. K., Talbot, W. A., McWhorter, T. J., & Wolf, B. O. (2019). The functional significance of facultative hyperthermia varies with body size and phylogeny in birds. *Functional Ecology*, *33*(4), 597–607. https://doi.org/10.1111/1365-2435.13274

Gerson, A. R., Smith, E. K., Smit, B., McKechnie, A. E., & Wolf, B. O. (2014). The Impact of Humidity on Evaporative Cooling in Small Desert Birds Exposed to High Air Temperatures. *Physiological and Biochemical Zoology*, *87*(6), 782–795. https://doi.org/10.1086/678956

Gleeson, M., & Brackenbury, J. H. (1984). EFFECTS OF BODY TEMPERATURE ON VENTILATION, BLOOD GASES AND ACID-BASE BALANCE IN EXERCISING FOWL. *Quarterly Journal of Experimental Physiology*, *69*(1), 61–72. https://doi.org/10.1113/expphysiol.1984.sp002796

Hackett, S. J., Kimball, R. T., Reddy, S., Bowie, R. C. K., Braun, E. L., Braun, M. J., Chojnowski, J. L., Cox, W. A., Han, K.-L., Harshman, J., Huddleston, C. J., Marks, B. D., Miglia, K. J., Moore, W. S., Sheldon, F. H., Steadman, D. W., Witt, C. C., & Yuri, T. (2008). A Phylogenomic Study of Birds Reveals Their Evolutionary History. *Science*, *320*(5884), 1763–1768. https://doi.org/10.1126/science.1157704

Hinds, D. S., & MacMillen, R. E. (1985). Scaling of Energy Metabolism and Evaporative Water Loss in Heteromyid Rodents. *Physiological Zoology*, *58*(3), 282–298. https://doi.org/10.1086/physzool.58.3.30155999

Hinds, D. S., & MacMillen, R. E. (1986). Scaling of Evaporative Water Loss in Marsupials. *Physiological Zoology*, *59*(1), 1–9. https://doi.org/10.1086/physzool.59.1.30156083

Hudson, D. M., & Bernstein, M. H. (1981). Temperature Regulation and Heat Balance in Flying White-necked Ravens, Corvus cryptoleucus. *Journal of Experimental Biology*, *90*(1), 267–281. https://doi.org/10.1242/jeb.90.1.267

Kleiber, M. (1932). Body size and metabolism. *Hilgardia*, *6*(11), 315–353. https://doi.org/10.3733/hilg.v06n11p315

Lemon, W. C. (1993). The Energetics of Lifetime Reproductive Success in the Zebra Finch Taeniopygia guttata. *Physiological Zoology*, *66*(6), 946–963. https://doi.org/10.1086/physzool.66.6.30163748

Lighton, J. R. (Sable S. I. (2008). *Measuring Metabolic Rates: A Manual for Scientists*. Oxford University Press.

Martin, T. E., Oteyza, J. C., Boyce, A. J., Lloyd, P., & Ton, R. (2015). Adult Mortality Probability and Nest Predation Rates Explain Parental Effort in Warming Eggs with Consequences for Embryonic Development Time. *The American Naturalist*, *186*(2), 223–236. https://doi.org/10.1086/681986

Martin, T. E., Riordan, M. M., Repin, R., Mouton, J. C., & Blake, W. M. (2017). Apparent annual survival estimates of tropical songbirds better reflect life history variation when based on intensive field methods. *Global Ecology and Biogeography*, *26*(12), 1386–1397. https://doi.org/10.1111/geb.12661

McKechnie, A. E., Gerson, A. R., & Wolf, B. O. (2021). Thermoregulation in desert birds: Scaling and phylogenetic variation in heat tolerance and evaporative cooling. *Journal of Experimental Biology*, *224*(Suppl_1), jeb229211. https://doi.org/10.1242/jeb.229211

McKechnie, A. E., & Lovegrove, B. G. (2002). Avian Facultative Hypothermic Responses: A Review. *The Condor*, *104*, 705–724. https://doi.org/10.1650/0010-5422(2002)104[0705:AFHRAR]2.0.CO;2

McNab, B. K. (1966). An Analysis of the Body Temperatures of Birds. *The Condor*,

68(1), 47–55. https://doi.org/10.2307/1365174

Muskett, P. C., Paterson, I. D., & Coetzee, J. A. (2020). Ground-truthing climate-matching predictions in a post-release evaluation. *Biological Control*, *144*, 104217. https://doi.org/10.1016/j.biocontrol.2020.104217

Myers, S. (2009). *Birds of Borneo: Brunei, Sabah, Sarawak, and Kalimantan*. Princeton University Press.

Noakes, M. J., Wolf, B. O., & McKechnie, A. E. (2016). Seasonal and geographical variation in heat tolerance and evaporative cooling capacity in a passerine bird. *Journal of Experimental Biology*, *219*(6), 859–869. https://doi.org/10.1242/jeb.132001

Pendar, H., & Socha, J. J. (2015). Estimation of instantaneous gas exchange in flow-through respirometry systems: A modern revision of bartholomew's ztransform method. *PLoS ONE*, *10*(10), 1–19. https://doi.org/10.1371/journal.pone.0139508

Pendar, H., Socha, J. J., & Chung, J. (2016). Recovering signals in physiological systems with large datasets. *Biology Open*, *5*(8), 1163–1174. https://doi.org/10.1242/bio.019133

Pollock, H. S., Brawn, J. D., Agin, T. J., & Cheviron, Z. A. (2019). Differences between temperate and tropical birds in seasonal acclimatization of thermoregulatory traits. *Journal of Avian Biology*, *50*(4), 1–11. https://doi.org/10.1111/jav.02067

Pollock, H. S., Brawn, J. D., & Cheviron, Z. A. (2021). Heat tolerances of temperate and tropical birds and their implications for susceptibility to climate warming. *Functional Ecology*, *35*(1), 93–104. https://doi.org/10.1111/1365-2435.13693

Prokosch, J., Bernitz, Z., Bernitz, H., Erni, B., & Altwegg, R. (2019). Are animals

shrinking due to climate change? Temperature-mediated selection on body mass in mountain wagtails. *Oecologia*, *189*(3), 841–849. https://doi.org/10.1007/s00442-019-04368-2

R Core Team. (2020). *R: A language and environment for statistical computing*. R Foundation for Statistical Computing. https://www.R-project.org/

Riddell, E. A., Iknayan, K. J., Hargrove, L., Tremor, S., Patton, J. L., Ramirez, R., Wolf, B. O., & Beissinger, S. R. (2021). Exposure to climate change drives stability or collapse of desert mammal and bird communities. *Science*, *371*(6529), 633–636. https://science.sciencemag.org/content/371/6529/633%0Ahttps://science.sciencemag.org/content/371/6529/633.abstract

Scholander, P. F., Hock, R., Walters, V., Johnson, F., & Irving, L. (1950). Heat regulation in some arctic and tropical mammals and birds. *The Biological Bulletin*, *99*(2), 237–258. https://doi.org/10.2307/1538741

Sheridan, J. A., & Bickford, D. (2011). Shrinking body size as an ecological response to climate change. *Nature Climate Change*, *1*(8), 401–406. https://doi.org/10.1038/nclimate1259

Slevin, M. C., Bin Soudi, E. E., & Martin, T. E. (2020). Breeding biology of the Mountain Wren-Babbler (Gypsophila crassus). *The Wilson Journal of Ornithology*, *132*(1), 124. https://doi.org/10.1676/1559-4491-132.1.124

Tieleman, B. I., Williams, J. B., & Bloomer, P. (2003). Adaptation of metabolism and evaporative water loss along an aridity gradient. *Proceedings of the Royal Society of London. Series B: Biological Sciences*, *270*(1511), 207–214. https://doi.org/10.1098/rspb.2002.2205

Torre-Bueno, J. R. (1978). *EVAPORATIVE COOLING AND WATER BALANCE DURING FLIGHT IN BIRDS*. 6.

Tucker, V. A. (1968). Respiratory Exchange and Evaporative Water Loss in the Flying Budgerigar. *Journal of Experimental Biology*, *48*, 67–87.

Van Buskirk, J., Mulvihill, R. S., & Leberman, R. C. (2010). Declining body sizes in North American birds associated with climate change. *Oikos*, *119*(6), 1047–1055. https://doi.org/10.1111/j.1600-0706.2009.18349.x

van Dyk, M., Noakes, M. J., & McKechnie, A. E. (2019). Interactions between humidity and evaporative heat dissipation in a passerine bird. *Journal of Comparative Physiology B*, *189*(2), 299–308. https://doi.org/10.1007/s00360-019-01210-2

Walsberg, G. E. (1993). Thermal Consequences of Diurnal Microhabitat Selection in a Small Bird. *Ornis Scandinavica*, *24*(3), 174. https://doi.org/10.2307/3676733

Walsberg, G. E., & Wolf, B. O. (1995). *VARIATION IN THE RESPIRATORY QUOTIENT OF BIRDS AND IMPLICATIONS FOR INDIRECT CALORIMETRY USING MEASUREMENTS OF CARBON DIOXIDE PRODUCTION*. *219*, 213–219.

Weathers, W. W. (1981). Physiological Thermoregulation in Heat-Stressed Birds: Consequences of Body Size. *Physiological Zoology*, *54*(3), 345–361. https://doi.org/10.1086/physzool.54.3.30159949

Weathers, W. W. (1997). Energetics and Thermoregulation by Small Passerines of the Humid, Lowland Tropics. *The Auk, 114*(3), 341–353. https://doi.org/10.2307/4089237

Weeks, B. C., Willard, D. E., Zimova, M., Ellis, A. A., Witynski, M. L., Hennen, M., &

Winger, B. M. (2020). Shared morphological consequences of global warming in North American migratory birds. *Ecology Letters*, *23*(2), 316–325. https://doi.org/10.1111/ele.13434

Whitfield, M. C., Smit, B., McKechnie, A. E., & Wolf, B. O. (2015). Avian thermoregulation in the heat: Scaling of heat tolerance and evaporative cooling capacity in three southern African arid-zone passerines. *Journal of Experimental Biology*, *218*(11), 1705–1714. https://doi.org/10.1242/jeb.121749

Withers, P. C. (1992). *Comparative animal physiology*. Saunders College Pub.

Wolf, B. O., & Walsberg, G. E. (1996a). Respiratory and cutaneous evaporative water loss at high environmental temperatures in a small bird. *Journal of Experimental Biology*, *199*(2), 451–457.

Wolf, B. O., & Walsberg, G. E. (1996b). Thermal Effects of Radiation and Wind on a Small Bird and Implications for Microsite Selection. *The Ecological Society of America*, *77*(7), 2228–2236.

A

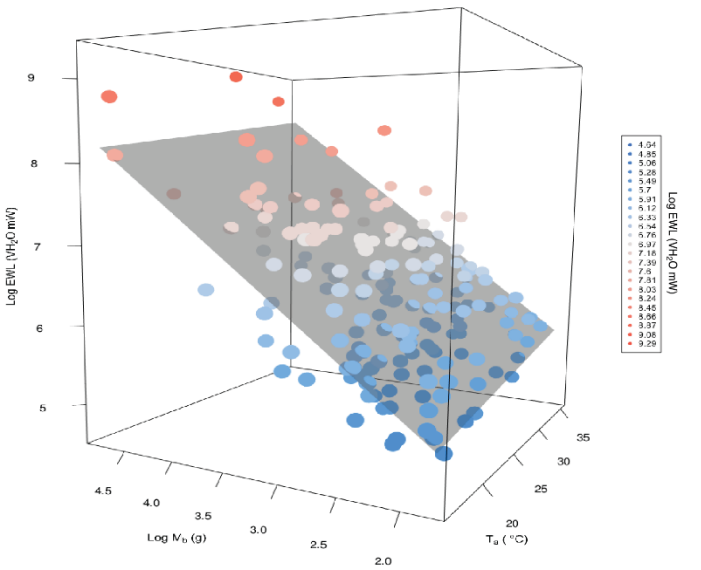
Log EWL (VH2O mW)
9
8
7
6
5
4.5
4.0
3.5
3.0
2.5
2.0
Log Mb (g)
20
25
30
35
Ta (°C)
Log EWL (VH2O mW)

B

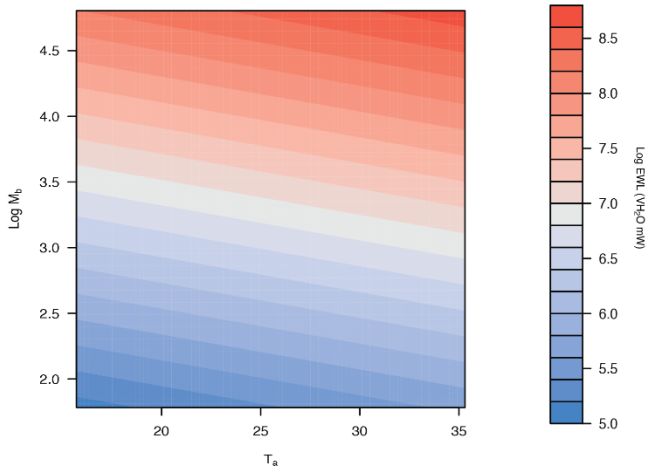
Log Mb
4.5
4.0
3.5
3.0
2.5
2.0
20
25
30
35
Ta
8.5
8.0
7.5
7.0
6.5
6.0
5.5
5.0
Log EWL (VH2O mW)

C

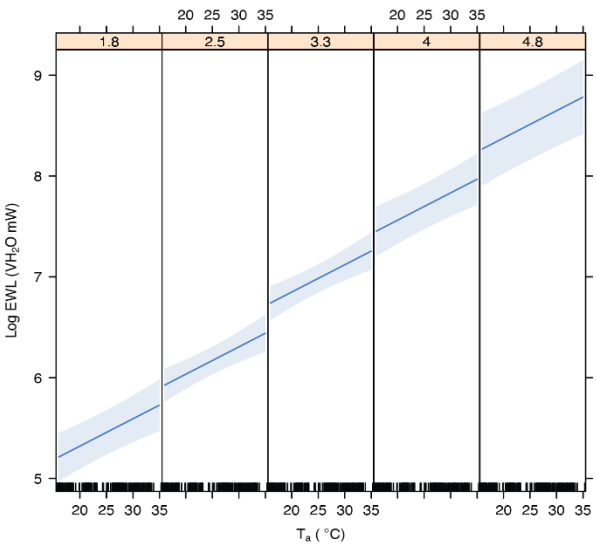
20 25 30 35
20 25 30 35
1.8
2.5
3.3
4
4.8
Log EWL (VH2O mW)
9
8
7
6
5
20 25 30 35
20 25 30 35
20 25 30 35
Ta (°C)

Figure 1. The predicted output of our model of exercise evaporative water loss ($EWL_{exercise}$) across body masses (M_b) and air temperature (T_a). Color indicates the $EWL_{exercise}$ values. The top graph (A) depicts the model prediction as the gray surface and the data that informed the model is represented by the colored points. The middle graph (B) represents only the model predictions. The bottom graph (C) depicts an effect plot where M_b is binned by quantiles.

Table 1. A summary table of our study species and their masses, BMR values and sample sizes used in our data analysis. (IOC World Bird List 12.1)

Species name	**Scientific name**	**Avg. Mb (g)**	**SD Mb (g)**	**Avg. BMR (mW)**	**BMR n**	**$MR_{exercise}$ n**
Bornean Stubtail	*Urosphena whiteheadi*	10.31	0.53	234.42	3	13
Bornean Whistler	*Pachycephala hypoxantha hypoxantha*	22.28	1.17	330.60	5	13
Bornean Whistling Thrush	*Myophonus borneensis*	116.80	5.40	927.21	7	5
Chestnut-crested Yuhina	*Staphida everetti*	13.00	1.02	212.18	18	29
Eyebrowed Jungle Flycatcher	*Vauriella gularis*	25.38	1.03	338.04	9	11
Grey-throated Babbler	*Stachyris nigriceps Borneensis*	15.91	1.34	236.40	13	16
Mountain Wren-Babbler	*Gypsophila crassa*	30.12	2.65	342.73	2	16
Penan Bulbul	*Alophoixus ruficrissus ruficrissus*	48.31	3.61	404.54	2	15
Snowy-browed Flycatcher	*Ficedula hyperythra mjobergi*	8.47	0.33	156.24	8	10
Temminck's Babbler	*Pellorneum pyrrogenys canicapillus*	18.95	1.10	335.19	11	17
White-throated Fantail	*Rhipidura albicollis kinabalu*	12.71	0.75	233.48	14	20

Yellow-breasted Warbler	*Phylloscopus montis montis*	6.54	0.33	134.12	7	22

A

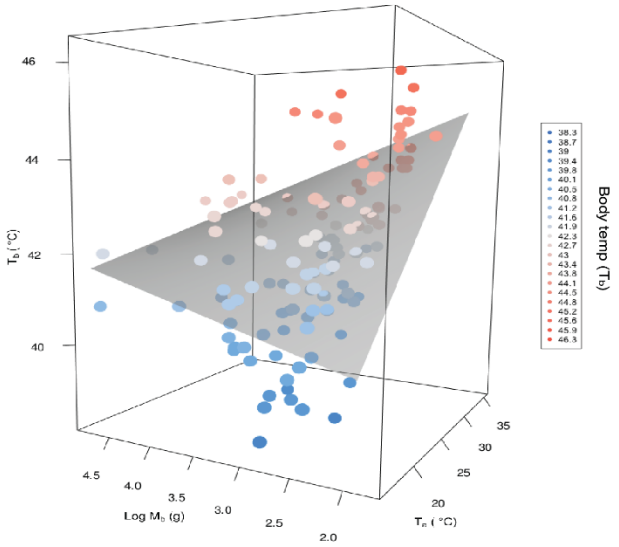
46
44
42
40
T_b (°C)
4.5
4.0
3.5
3.0
2.5
2.0
Log M_b (g)
35
30
25
20
T_a (°C)
Body temp (T_b)

B

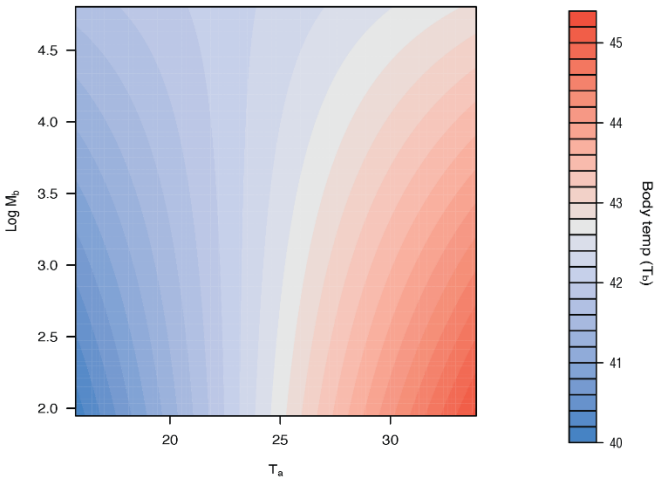
4.5
4.0
3.5
3.0
2.5
2.0
Log M_b
20
25
30
T_a
45
44
43
42
41
40
Body temp (T_b)

C

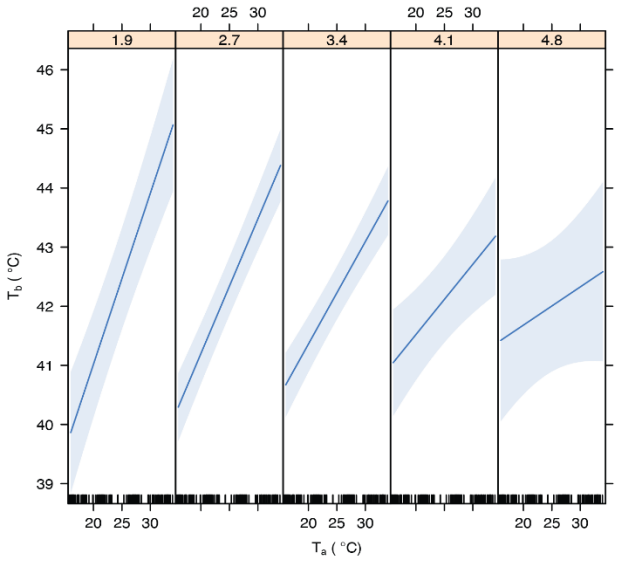
20 25 30
20 25 30
1.9
2.7
3.4
4.1
4.8
46
45
44
43
42
41
40
39
T_b (°C)
20 25 30
20 25 30
20 25 30
T_a (°C)

Figure 2. The predicted output of our model of exercise Body Temperature ($T_{b\ exercise}$) across body masses (M_b) and air temperature (T_a). Color indicates the $T_{b\ exercise}$ values corresponding to the gradient bar displayed on the right of the graphs. The top graph (A) depicts the model prediction as the gray surface and the data that informed the model is represented by the colored points. The bottom graph (B) represents only the model predictions. The bottom graph (C) depicts an effect plot where M_b is binned by quantiles.

A

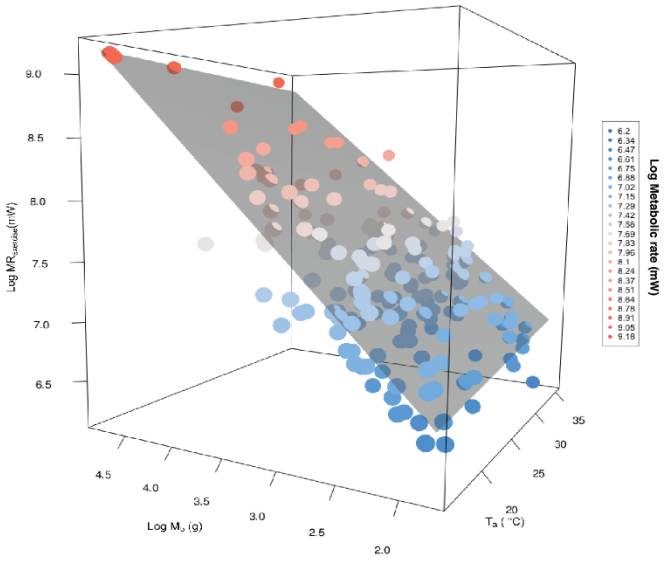
Log MR$_{exercise}$(mW)
9.0
8.5
8.0
7.5
7.0
6.5
4.5
4.0
3.5
3.0
2.5
2.0
Log M$_b$ (g)
20
25
30
35
T$_a$ (°C)
Log Metabolic rate (mW)
6.2
6.34
6.47
6.61
6.75
6.88
7.02
7.15
7.29
7.42
7.56
7.69
7.83
7.96
8.1
8.24
8.37
8.51
8.64
8.78
8.91
9.05
9.18

B

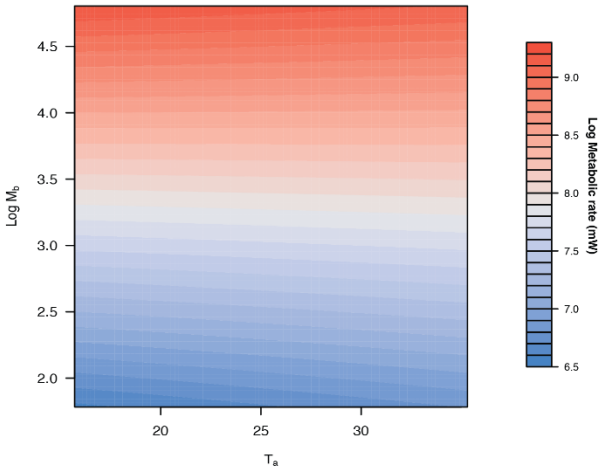
Log M$_b$
4.5
4.0
3.5
3.0
2.5
2.0
20
25
30
T$_a$
Log Metabolic rate (mW)
9.0
8.5
8.0
7.5
7.0
6.5

C

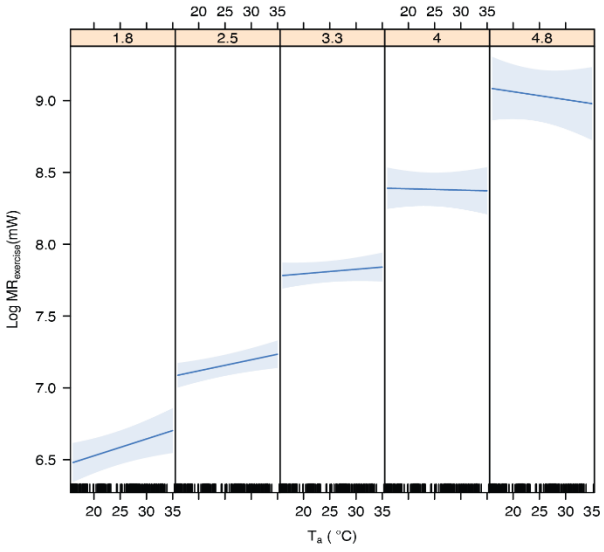
20 25 30 35
20 25 30 35
1.8
2.5
3.3
4
4.8
Log MR$_{exercise}$(mW)
9.0
8.5
8.0
7.5
7.0
6.5
20 25 30 35
20 25 30 35
20 25 30 35
T$_a$ (°C)

Figure 3. The predicted output of our model of exercise metabolic rate ($MR_{exercise}$) across body masses (M_b) and air temperature (T_a). Color indicates the $MR_{exercise}$ values corresponding to the gradient bar displayed on the right of the graphs. The top graph (A) depicts the model prediction as the gray surface and the data that informed the model is represented by the colored points. The bottom graph (B) represents only the model predictions. The bottom graph (C) depicts an effect plot where M_b is binned by quantiles.

A

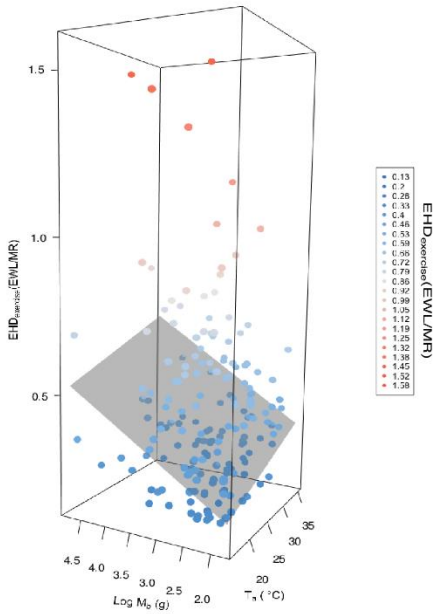
1.5
1.0
0.5
EHD exercise (EWL/MR)
4.5
4.0
3.5
3.0
2.5
2.0
Log M_b (g)
20
25
30
35
T_a (°C)
EHD exercise (EWL/MR)

B

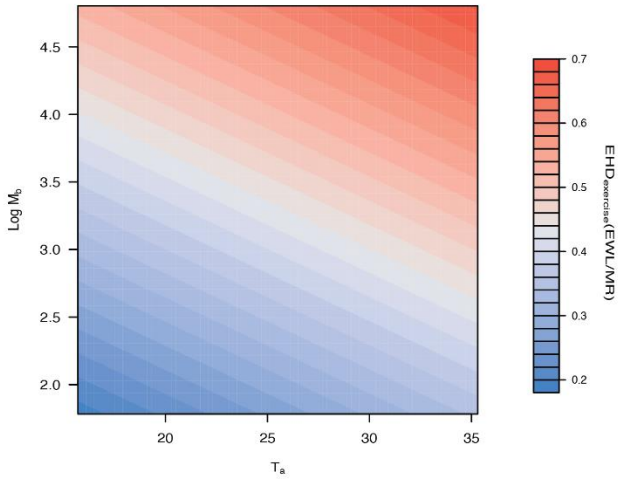
4.5
4.0
3.5
3.0
2.5
2.0
Log M_b
20
25
30
35
T_a
0.7
0.6
0.5
0.4
0.3
0.2
EHD exercise (EWL/MR)

C

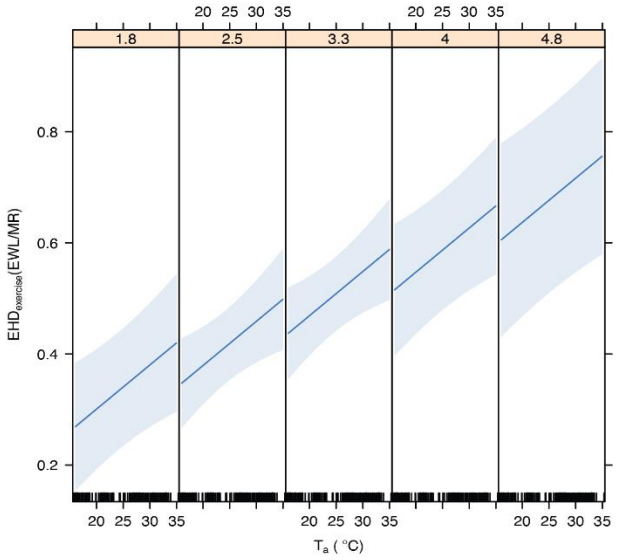
20 25 30 35
20 25 30 35
1.8
2.5
3.3
4
4.8
0.8
0.6
0.4
0.2
EHD exercise (EWL/MR)
20 25 30 35
20 25 30 35
20 25 30 35
T_a (°C)

Figure 4. The predicted output of our model of exercise evaporative heat dissipation ($EHD_{exercise}$) across body masses (M_b) and air temperature (T_a). Color indicates the $MR_{exercise}$ values corresponding to the gradient bar displayed on the right of the graphs. The top graph (A) depicts the model prediction as the gray surface and the data that informed the model is represented by the colored points. The bottom graph (B) represents only the model predictions. The bottom graph (C) depicts an effect plot where M_b is binned by quantiles.

Table 2. A summary table of all model ANOVA outputs. Where the top row indicates the response variable for each model.

	Log $EWL_{exercise}$			T_b			Log $MR_{exercise}$			$EHD_{exercise}$		
Predictors	*Estimates*	*CI*	*p*	*Estimates*	*CI*	*p*	*Estimates*	*CI*	*p*	*Estimates*	*CI*	*p*
(Intercept)	2.58	1.99 – 3.18	<0.001	31.86	27.30 – 36.42	<0.001	4.28	3.69 – 4.88	<0.001	-0.06	-0.34 – 0.22	0.670
T_a	0.03	0.02 – 0.04	<0.001	0.44	0.26 – 0.61	<0.001	0.02	0.00 – 0.04	0.050	0.01	0.00 – 0.01	0.008
Log M_b	1.02	0.85 – 1.19	<0.001	1.78	0.31 – 3.24	0.018	0.96	0.76 – 1.16	<0.001	0.11	0.03 – 0.19	0.007
hops	0.01	0.00 – 0.02	0.005				0.01	0.00 – 0.01	<0.001			
T_a * Log M_b				-0.08	-0.13 – -0.02	0.007	-0.01	-0.01 – 0.00	0.142			
Random Effects												
σ^2	0.20			1.10			0.04			0.05		
τ_{00}	0.03 $_{species}$			0.33 $_{species}$			0.01 $_{species}$			0.01 $_{species}$		
ICC	0.13			0.23			0.20			0.11		
N	12 $_{species}$			11 $_{species}$			12 $_{species}$			12 $_{species}$		
Observations	187			135			187			187		
Marginal R^2 / Conditional R^2	0.685 / 0.725			0.491 / 0.608			0.865 / 0.891			0.111 / 0.209		

APPENDICES

Appendix A. The top graph (A) depicts the raw, transformed, and baseline/calibration CO_2 values of a calibration trial conducted in the lab with the wheel in motion. The bottom graph (B) depicts the raw, transformed, and baseline/calibration H_2O values of the same calibration trial conducted in the lab with the wheel in motion. The green shading represents the 5 minute period in which we would be sampling if this were an animal trial. The gray shaded area represents the selected values using the same methods of selection for the animal trials.

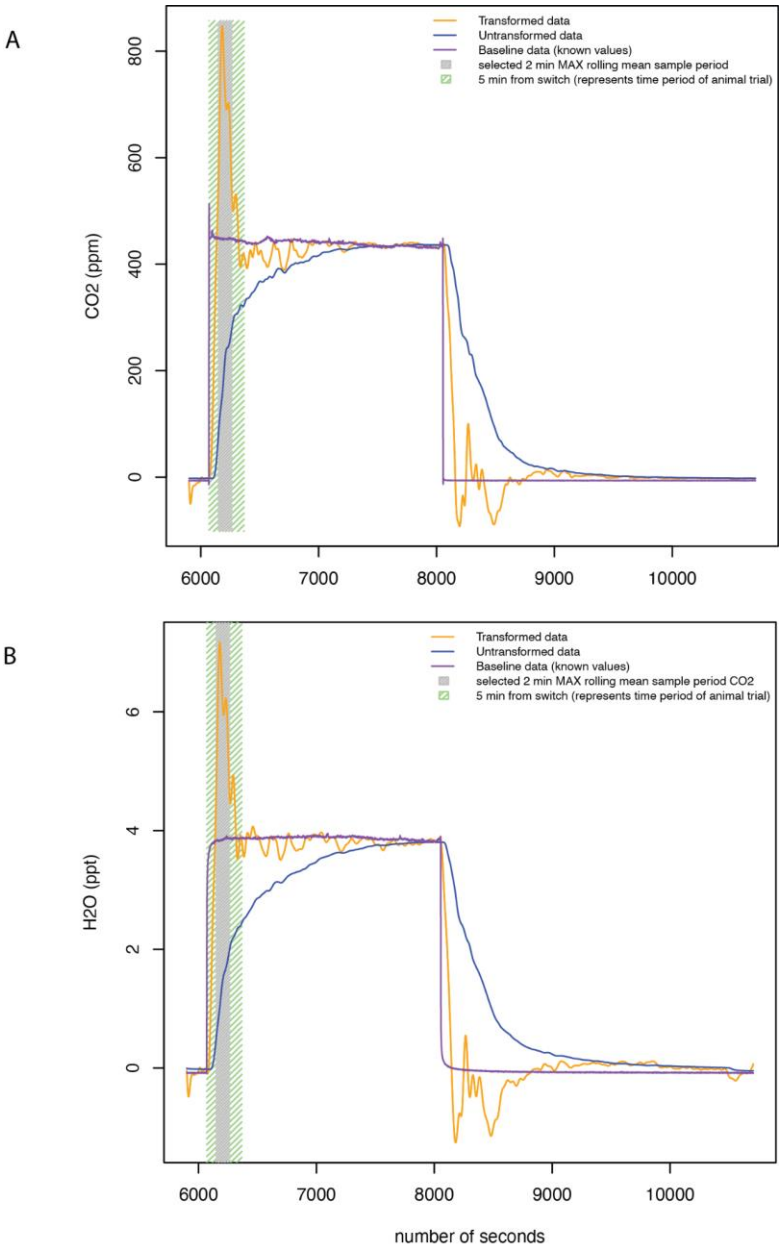

Appendix B: Example of transformed data from a trial of a White-throated Fantail at 27°C. The top panel is CO_2 measurement and the bottom panel is H_2O measurements. Black line indicates transformed values, blue line indicates raw values, pink dots are body temperature measurements, and red dots are hops measurements. Vertical lines indicate the start and stop of the exercise trial while orange regions indicate the potential sample period and the green regions indicate the selected sample period.

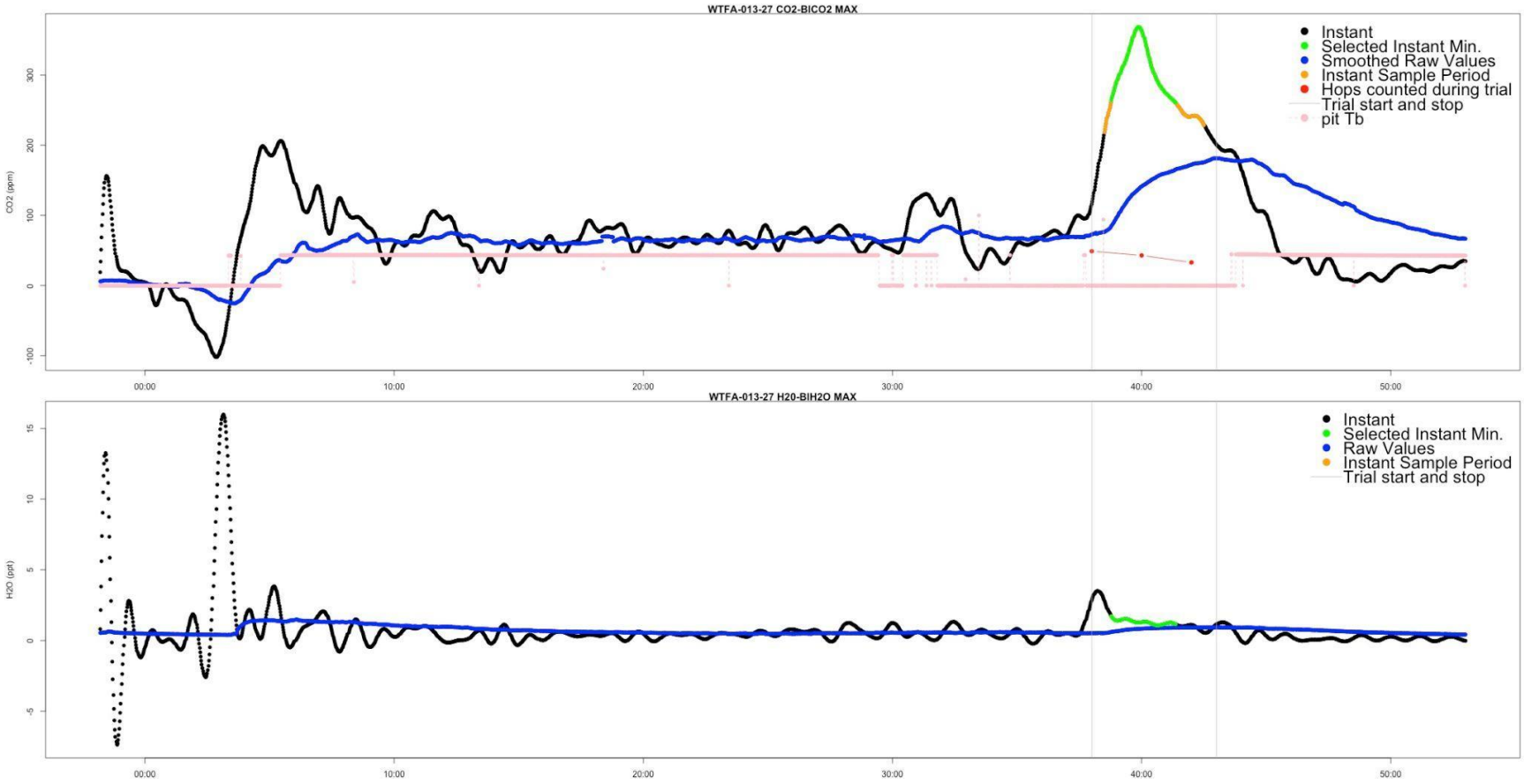

Appendix C: Model selection of log exercise evaporative water loss rates ($EWL_{exercise}$) as the response variable.

Model	Class	K	log $\mathscr{L}$	AIC	ΔAIC	w_i
log EWL ~ T_a + log M_b + hops + (1 | speices)	lmerMod	6	-122.441	256.881	0.000	0.917
log EWL ~ T_a + log M_b + (1 | speices)	lmerMod	5	-126.177	262.353	5.472	0.059
log EWL ~ T_a * log M_b + (1 | speices)	lmerMod	6	-126.128	264.256	7.374	0.023
log EWL ~ T_a + log M_b	lm	4	-134.721	277.443	20.561	0.000
log EWL ~ T_a * log M_b	lm	5	-134.497	278.994	22.113	0.000
log EWL ~ log M_b	lm	3	-141.918	289.837	32.955	0.000
log EWL ~ T_a	lm	3	-228.550	463.100	206.219	0.000

Appendix D: Model selection of body temperature as the response variable.

Model	Class	K	log $\mathscr{L}$	AIC	ΔAIC	w_i
$T_{b\ exercise} \sim T_a * M_b + (1 \mid species)$	lmerMod	6	-205.893	423.785	0.000	0.911
$T_{b\ exercise} \sim T_a + M_b + (1 \mid species)$	lmerMod	5	-209.551	429.102	5.317	0.064
$T_{b\ exercise} \sim T_a + M_b + hops + (1 \mid species)$	lmerMod	6	-209.480	430.960	7.175	0.025
$T_{b\ exercise} \sim T_a * M_b$	lm	5	-215.012	440.025	16.240	0.000
$T_{b\ exercise} \sim T_a$	lm	3	-217.972	441.944	18.159	0.000
$T_{b\ exercise} \sim T_a + M_b$	lm	4	-217.888	443.776	19.991	0.000
$T_{b\ exercise} \sim M_b$	lm	3	-260.057	526.113	102.328	0.000

Appendix E: Model selection of Metabolic rate as the response variable.

Model	Class	K	log $\mathscr{L}$	AIC	ΔAIC	w_i
$\log MR_{exercise} \sim T_a * \log M_b + hops + (1 \mid speices)$	lmerMod	7	29.1769	-44.3537	0.0000	0.5208
$\log MR_{exercise} \sim T_a + \log M_b + hops + (1 \mid speices)$	lmerMod	6	28.0936	-44.1872	0.1665	0.4792
$\log MR_{exercise} \sim T_a + \log M_b + (1 \mid speices)$	lmerMod	5	17.5254	-25.0507	19.3030	0.0000
$\log MR_{exercise} \sim T_a * \log M_b + (1 \mid speices)$	lmerMod	6	18.3227	-24.6454	19.7084	0.0000
$\log MR_{exercise} \sim T_a * \log M_b$	lm	5	12.4902	-14.9804	29.3734	0.0000
$\log MR_{exercise} \sim T_a * \log M_b$	lm	4	11.4666	-14.9333	29.4204	0.0000
$\log MR_{exercise} \sim \log M_b$	lm	3	9.6175	-13.2350	31.1187	0.0000
$\log MR_{exercise} \sim T_a$	lm	3	-159.7216	325.4431	369.7969	0.0000

Appendix F: Model selection of evaporative heat dissipation as the response variable.

Model	Class	K	log $\mathscr{L}$	AIC	ΔAIC	w_i
$EHD_{exercise} \sim T_a + \log M_b + (1 \mid speices)$	lmerMod	5	4.351	1.298	0.000	0.436
$EHD_{exercise} \sim T_a * \log M_b + (1 \mid speices)$	lmerMod	6	4.995	2.011	0.712	0.305
$EHD_{exercise} \sim T_a + \log M_b + hops + (1 \mid speices)$	lmerMod	6	4.715	2.570	1.271	0.231
$EHD_{exercise} \sim T_a + \log M_b$	lm	4	-0.313	8.626	7.328	0.011
$EHD_{exercise} \sim \log M_b$	lm	4	-0.313	8.626	7.328	0.011
$EHD_{exercise} \sim T_a * \log M_b$	lm	5	-0.034	10.069	8.770	0.005
$EHD_{exercise} \sim T_a$	lm	3	-7.366	20.731	19.433	0.000

Appendix G: Pagel's lambda and Blomberg's K results for subsets of the data at high (≥ 27°C) and low temperatures (≤ 19°C) for BMR, $MR_{exercise}$, $T_{b\ exercise}$, and $EWL_{exercise}$.

variable	lambda_pvalue	lambda_value	blomberg_pvalue	blomberg_k
low_temps_BMR_mW_g	1.0000000	0.00004592065	0.354	0.6470587
low_temps_BMR_mean	1.0000000	0.00004592065	0.757	0.4755113
low_temps_tb_mean	1.0000000	0.00004592065	0.873	0.4553122
low_temps_EWL_mW_g_mean	1.0000000	0.00004592065	0.511	0.5890128
low_temps_EWL_mean	1.0000000	0.00004592065	0.831	0.4559118
low_temps_MR_mW_g_mean	0.9170729	0.09695668683	0.242	0.7073467
low_temps_MR_mean	1.0000000	0.00004592065	0.818	0.4623125
high_temps_BMR_mW_g	1.0000000	0.00004592065	0.362	0.6470587
high_temps_BMR_mean	1.0000000	0.00004592065	0.751	0.4755113
high_temps_tb_mean	1.0000000	0.00004592065	0.704	0.5127891
high_temps_EWL_mW_g_mean	1.0000000	0.00004592065	0.684	0.5290474

high_temps_EWL_mean	1.0000000	0.00004592065	0.777	0.4705129
high_temps_MR_mW_g_mean	1.0000000	0.00004592065	0.942	0.4310975
high_temps_MR_mean	1.0000000	0.00004592065	0.757	0.4821799